SUB- AND SUPERCRITICAL BIFURCATIONS AND TURNING POINTS IN A SIMPLE BWR MODEL

Rizwan-uddin♦
Department of Nuclear, Plasma and Radiological Engineering
University of Illinois at Urbana-Champaign
Urbana, IL, 61801, USA
rizwan@uiuc.edu

ABSTRACT

Stability and bifurcation analyses of BWRs have been performed using a reduced order, nuclear-coupled thermal hydraulics model. This has been carried out using a bifurcation analysis code, BIFDD. A large segment of the parameter space has been investigated using this very efficient tool. Stability boundaries are obtained in several two-dimensional parameter spaces. In addition, the nature of bifurcation along these stability boundaries has also been determined. Results indicate that both subcritical as well as supercritical Poincaré-Andronov-Hopf bifurcations are likely to occur in regions of interest in parameter space.

In addition to the semi-analytical bifurcation studies, the governing equations have also been integrated numerically. Results confirm the findings of the bifurcation analysis. Numerical integrations, carried out for parameter values away from the stability boundary, further show that the bifurcation curves, in many cases of subcritical bifurcations, have a turning point. The bifurcation curve in these cases extends back into the unstable region. These results show that it is possible to experience *large amplitude stable oscillations* in the unstable region infinitesimally close to the stability boundary. Moreover, *large amplitude stable oscillations* are also possible in the stable region of the parameter space near the stability boundary, following large but finite perturbations. These findings provide alternate explanation for the experimental and operational observations in BWRs that indicate the existence of stable limit cycle oscillations and the possibility of growing amplitude oscillations.

Results obtained here using a simple model suggest that further work along these lines, with more detailed models, is needed to identify operating conditions and perturbation amplitudes that might lead to stable limit cycles or growing amplitude oscillations in current and next generation of BWRs.

♦ Also, Computational Science and Engineering Program, University of Illinois at Urbana-Champaign.

1. INTRODUCTION

Instabilities associated with two-phase flow as well as the feedback mechanism between neutronics and thermal hydraulics specific to boiling water reactors (BWRs) make nuclear-coupled thermal hydraulics (NCTH) analyses of current and next generation BWRs an important research goal [1-3]. Today, as a result of the concerted effort that started following some of the early instability incidents in BWRs, instabilities related to nuclear-coupled thermal hydraulics are much better understood. Despite significant development in the understanding of these instabilities and in system codes capable of simulating them, new incidents continue to be reported (Laguna Verde power plant in 1995 [4]; Oskarshamn-3 in 1998 [5]). Though there are some common features, each incident is, in general, unique, caused by a unique set of conditions. Hence, there is continued need to develop better fundamental understanding of possible instability scenarios, and conditions that lead to them. Such an understanding will provide guidance in classification of events in BWRs, and help in developing guidelines to avoid them.

Past work has identified two features of NCTH instabilities in BWRs that are relevant to event classification purposes. First; BWRs can experience in-phase (core wide) or out-of-phase (regional) NCTH oscillations [6]. Second; some NCTH instabilities in operating reactor cores and in controlled experiments in BWRs have resulted in stable, finite amplitude oscillations [4, 7, 8], while others lead to oscillations with growing amplitude, until stopped by automatic or manual scram [5, 9]. While in-phase and out-of-phase oscillations can be predicted by linear analysis using a detailed model of the core physics, analysis of the second phenomenon—which has received less attention in the past—necessarily requires the set of nonlinear equations either integrated numerically or studied using analytical bifurcation techniques. Focus of this work is to identify possible scenarios within this second feature of NCTH instabilities. Namely, to identify conditions that lead to stable or unstable oscillations; characteristics of the resulting oscillations; and to study the effect of initial conditions on the state to which the BWR evolves.

In general there have been three approaches to analyze nuclear-coupled thermal hydraulics instabilities in BWRs:

1) Time domain numerical simulations carried out using *large scale,* high-fidelity codes such as RAMONA, TRAB-BWR, TRACG, RETRAN, TOSDYN-2, RELAP/PANBOX [10-20], and others discussed in Ref. 1.
2) Frequency domain analyses performed using codes such as LAPUR, MATSTAB, NUFREQ-NP, STAIF [4, 6, 21-23] etc., or using low dimensional models [24-28].
3) Bifurcation analyses usually carried out with low-dimensional models that are obtained after reducing the set of governing partial differential equations (PDEs) to a set of ordinary differential equations (ODEs) [24, 29-33].

Since the goal of the current work is to identify and distinguish possible instability scenarios and characteristics of the resulting oscillations, frequency domain analysis is an important first step. It however only provides limited information. Time domain numerical simulations using detailed

models over large regions of the multi-dimensional parameter space can provide detailed behavior of the system dynamics. These, however, are very laborious and not very practical for parametric studies. Hence, the approach used here is to perform extensive semi-analytical bifurcation analyses using a low dimensional model of BWR and—guided by the results of these analyses—perform limited numerical simulations to confirm and extend the results of the former.

For this purpose a reduced order model has been used. This model [34] has been used earlier by March-Leuba, Cacuci and Perez [29] and Muñoz-Cobo and Verdú [30]. Current work exploits the efficiency of general-purpose bifurcation and dynamical system codes to explore semi-analytically and numerically much larger regions in parameter space than studied earlier. Consequently, both sub- and supercritical bifurcations, and turning points in bifurcation diagrams have been found in some regions of parameter space. These regions are not far from those studied earlier [29, 30] that had shown the existence of only supercritical bifurcations. (Model used here employs only the point reactor kinetics equations for reactor physics, and hence is incapable of simulating out-of-phase oscillations.)

It is realized that the use of a simple model will not allow quantitative conclusions to be made. However, results obtained here and conclusions reached based on those results, will allow and guide the users of system codes—codes that are more faithful to actual physics—to better understand and interpret their results. In addition, these results will also help in better characterization of oscillations measured in BWRs.

2. BACKGROUND

This section is divided into two parts. A review of related mathematical background and mathematically possible scenarios is given first. Next, past work on bifurcation analysis of BWRs is reviewed and analyzed.

2.1 MATHEMATICAL BACKGROUND

Existence of stable or unstable periodic solutions to a set of nonlinear ordinary differential equations (a dynamical system) was proved by Hopf [35]. Recognizing earlier contributions by Poincaré and Andronov, the theorem is sometimes called Poincaré-Andronov-Hopf (PAH) bifurcation theorem [36]. This theorem guarantees the existence of periodic (stable or unstable) solutions to nonlinear differential equations if certain conditions are satisfied [37-41].

Poincaré-Andronov-Hopf Bifurcation

The theorem statement is reproduced below from Ref. [41]. Consider an autonomous system of ODEs

$$\frac{d\underline{x}}{dt} = F(\underline{x}, \lambda) \tag{1}$$

where F: R^n x $R \rightarrow R^n$ is C^∞ and λ is the bifurcation parameter. Suppose that

$$F(0,\lambda) \equiv 0. \tag{2}$$

So, $\underline{x} = 0$ is a steady-state solution (or fixed point) to Eq. (1) for all λ. Let $A(\lambda) = (dF)_{0,\lambda}$ be *the n* x *n* Jacobian matrix of F along the steady-state solutions, and

(H-1): $A(\lambda = \lambda_c)$ has simple eigenvalues $\pm i\omega$, and no other eigenvalues lying on the imaginary axis.
(H-2): The eigenvalues of $A(\lambda)$ are of the form $\sigma(\lambda) \pm i\omega(\lambda)$ and $d\sigma(\lambda = \lambda_c)/d\lambda \neq 0$, i.e., the real parts of the eigenvalues of $A(\lambda)$ cross the imaginary axis with non-zero speed as λ crosses λ_c.

If Eq. (1) satisfies (H-1) and (H-2) then there is an $(L+1)$-parameter family of periodic orbits of Eq. (1) bifurcating from the steady-state solution $\underline{x} = 0$ at $\lambda = \lambda_c$, where L is the number of auxiliary parameters besides λ.

Although the original proof by Hopf involved *ad-hoc* asymptotic analysis techniques, the theorem can be proved by a direct application of the center manifold theorem and normal form theorem as given in Refs. 38 and 41. The theorem also has been extended to classes of PDEs and functional differential equations [37, 38, 41, 42]. Detailed analysis of the theorem shows that the periodic solutions exist for either $\lambda > \lambda_c$, or $\lambda < \lambda_c$ or $\lambda = \lambda_c$. For the case when all the eigenvalues of $A(\lambda)$ have negative real parts for $\lambda > \lambda_c$ (i.e., if $\lambda > \lambda_c$ is the stable region), the periodic solutions are stable if they exist for $\lambda < \lambda_c$, and unstable if they exist for $\lambda > \lambda_c$. Stability for $\lambda = \lambda_c$ case is not, in general, determined automatically by the PAH theorem. The stability of the periodic solutions is determined by the Floquet theory of differential equations with periodic coefficients [35, 41]. Floquet theory is based on linear analysis and hence, stable solutions obtained as a result of invoking the PAH bifurcation are proven to be stable only for small perturbations.

In simpler terms the theorem implies that periodic solutions to the nonlinear differential equations exist for parameter values λ if at $\lambda = \lambda_c$ a pair of complex conjugate eigenvalues of the Jacobian matrix has zero real part while all others are away from, and to the left of, the imaginary axis, and the derivative of the real part of the pair of eigenvalues on the imaginary axis with respect to λ is non-zero. These periodic solutions only exist either on the stable side (all eigenvalues with negative real parts) or on the unstable side (one pair of complex conjugate eigenvalues with positive real parts). Transition from a fixed point to a fixed point and a periodic solution (limit cycle), for the case when $\lambda > \lambda_c$ is the stable region, is shown schematically in Fig. 1(a,b). The case of subcritical PAH bifurcation, shown in Fig. 1(a), has unstable periodic solutions (repeller limit cycles) for $\lambda > \lambda_c$. Hence, for $\lambda > \lambda_c$ perturbations of amplitude less than the amplitude of the parabola will decay to zero and perturbations of amplitude greater than the limit cycle amplitude will be repelled by the limit cycle and hence will move away from the steady-state "stable" fixed point as well as from the unstable limit cycle. Hence, in this case the fixed point will be stable for sufficiently small perturbations. On the other hand, in the supercritical PAH bifurcation case, shown in Fig. 1(b), there exist stable limit cycles in the unstable region, and hence small perturbations grow and stabilize at the limit cycle, while perturbations with amplitude larger than the limit cycle radius can decay onto

the limit cycle, depending upon the size of the perturbation and the basin of attraction of the stable limit cycle.

In summary, crossing a stability boundary between a region with no eigenvalues with positive real parts and a region with one pair of complex conjugate eigenvalues with positive real parts implies PAH bifurcation. Such a stability boundary can be easily determined via a linear analysis. However, to determine the nature of the bifurcation (sub- vs. supercritical) and to determine the oscillation amplitude close to the stability boundary, additional (bifurcation) analyses are necessary. Such bifurcation studies are usually performed in one of two ways: by numerically integrating the set of governing equations or analytically. Numerical methods and codes for numerical integration of set of ODEs are well known. Software packages are also available for PCs that allow efficient determination of parametric dependence and the effects of initial conditions. Second approach—analytical bifurcation—often involves some form of asymptotic expansion method, one of which is explained below. (An alternative analytical approach is to reduce the model to the Poincaré normal form via the center manifold theorem.)

Lindstedt-Poincaré Asymptotic Expansion Analysis

In this technique, to account for the frequency dependence on the nonlinear terms, both, the dependent variable $\underline{x}$ as well as the frequency ω are expanded in powers of a small parameter ε as [40]

$$\underline{x} = \varepsilon \underline{x}_1 + \varepsilon^2 \underline{x}_2 + \varepsilon^3 \underline{x}_3 + ... \tag{3}$$

$$1/\omega = 1/\omega_0 + \varepsilon\tau_1 + \varepsilon^2\tau_2 + ... \tag{4}$$

By defining a new time θ as, $\theta = \omega t$, the relationship between t and θ becomes

$$t = (1/\omega_0 + \varepsilon\tau_1 + \varepsilon^2\tau_2 + ...)\theta \tag{5}$$

Equation (5), when used in the asymptotic analysis, takes into account the correction in frequency. The coefficients τ_i *(i = 1, 2, 3,...)* are determined in the course of the analysis by requiring the expansion of $\underline{x}$ to be uniform for all θ.

In general there may not be a relevant small parameter in the description of the NCTH problem, and hence, one must be introduced. Realizing that the asymptotic analysis is carried out by perturbing about the solution on the stability boundary and it will hence be valid only for operating points near the stability boundary, a small quantity μ is defined as the distance parallel to the bifurcation axis from the operating point to the stability boundary. For example, in the a - λ space in Fig. 2

$$\mu = \lambda_{op.pt} - \lambda_c \tag{6}$$

where λ is the bifurcation parameter and a is any other parameter. Here, for a given set of values of other parameters, $\lambda_{op.\ pt}$ is the value of the bifurcation parameter at the operating point near the

stability boundary, and λ_c is its value on the stability boundary. The parameter μ, following the PAH theorem, is an analytic function of ε and can be expanded as

$$\mu = \varepsilon\mu_1 + \varepsilon^2\mu_2 + ... \tag{7}$$

Substituting Eq. (7) in Eq. (6) yields

$$\lambda_{op.pt} = \lambda_c + (\varepsilon\mu_1 + \varepsilon^2\mu_2 + ...) \tag{8}$$

The parameter that determines the stability of the periodic solutions, β (which is different from the same symbol used later for the fraction of delayed neutrons) is also similarly expanded in powers of ε

$$\beta = \varepsilon\beta_1 + \varepsilon^2\beta_2 + ... \tag{9}$$

Details of the analysis involve substitution of the above equations into Eq. (1) leading to a hierarchy of equations in powers of ε, and repeated application of the Fredholm alternative theorem. The parameters μ_1, τ_1 and β_1 are found to be identically zero. Hence, μ_2, τ_2 and β_2 are evaluated to determine the nature of the bifurcation. Truncating the expansions at the second order allows the evaluation of the oscillation amplitude ε from

$$\varepsilon \approx \sqrt{\frac{\mu}{\mu_2}} = \sqrt{\frac{\lambda_{op.pt} - \lambda_c}{\mu_2}} \tag{10}$$

Moreover, the first order solution for the first component in $\underline{x}$ is given by

$$x_1 = \varepsilon \cos(\theta) \tag{11}$$

Evaluation of μ_2, τ_2 and β_2, even for reduced order simple models, is a very tedious task and quickly becomes almost impossible with increasing order of the model. Another drawback of the analytical bifurcation studies is that each is specific to a bifurcation parameter, and must be repeated if the impact of a different parameter is to be studied. Due to the limitations on the two approaches (numerical integration and analytical bifurcation studies), there has been limited investigation of the large parameter space even in simple models of BWRs.

Semi-Analytical Local Bifurcation Analysis

Analytical bifurcation carried out *numerically* is an attractive alternative to the two approaches described above. In this approach the governing set of nonlinear equations are neither integrated numerically in time nor treated entirely analytically. Rather, the *analytical reduction* to the Poincaré normal form via the center manifold theorem is carried out *numerically* [43, 44]. This approach,

which will henceforth be called the *analytic-numeric approach*, allows accurate and efficient evaluation of the entire parameter space of interest. General-purpose bifurcation codes such as BIFDD [44] have been developed to perform analytic-numeric bifurcation analysis of set of ODEs and ODEs with delays. For a given set of nonlinear ODEs (or ODEs with delays) and the corresponding Jacobian matrix, the code determines the critical value of the bifurcation parameter, nature of the bifurcation, and the oscillation amplitude when operating close to the critical value. BIFDD allows any parameter of choice in the model to be selected as the bifurcation parameter, and hence the entire parameter space can easily be spanned.

Bifurcation analysis when carried out analytically or via an analytic-numeric approach, yields—for all other parameters fixed—the critical value of the bifurcation parameter $\lambda = \lambda_c$, frequency of oscillation ω_0 corresponding to the critical value, and parameters μ_2 , τ_2 and β_2. A negative (positive) value of β_2 indicates a supercritical (subcritical) PAH bifurcation, i.e., stable (unstable) limit cycle oscillations as the bifurcation parameter is varied across the critical value. τ_2 is a correction factor to the oscillation frequency, and μ_2 relates the oscillation amplitude to the value of the bifurcation parameter through Eq. (10). In the immediate vicinity of the critical value, PAH bifurcation theorem predicts the oscillation amplitude to rise as $(\lambda - \lambda_c)^{1/2}$

By incrementally varying a second parameter and repeating the calculations for the critical value of the bifurcation parameter, one can easily generate stability boundaries and determine the nature of the bifurcation along those boundaries in two-dimensional parameter spaces. This can further be extended easily to generate stability-surfaces in three or higher dimensional parameter spaces.

Beyond (Local) Bifurcation

As stated earlier, PAH theorem is based on linear analysis. Moreover, the stability of the resulting limit cycle is determined using a linear (Floquet) theory. Hence, these results are valid only for parameter values close to the stability boundary (where the small parameter is *small*), and for small perturbations. System dynamics away from the stability boundary can be determined by numerically integrating the set of nonlinear ODEs. Results obtained using numerical integration can be used to estimate the width of the strip adjacent to the stability boundary over which the (local) analytical bifurcation results are valid. Numerical integrations also predict additional (global) system dynamics that cannot be predicted by local techniques. For example, in some cases, the bifurcation curve may have one or more turning points. One such diagram for subcritical bifurcation is shown in Fig. 3. The bifurcation diagram, in this case, has a turning point at $\lambda = \lambda_{c,t}$. Hence, for $\lambda > \lambda_{c,t}$, the unstable periodic solutions predicted by the PAH theorem cease to exist. Instead a branch of stable periodic solutions exists on top of the unstable branch predicted by the PAH theorem. This suggests that even in the stable region close to the stability boundary (before the turning point), after a large enough perturbation, the system would evolve to large amplitude stable limit cycle. Hence, it provides assurance that the rising amplitude oscillations predicted by the PAH theorem under these conditions are actually bounded and saturate at a stable limit cycle. Also, in this case, the system when operating in the unstable region infinitesimally close to the stability boundary will evolve to large amplitude stable oscillations. One difference between such a subcritical case (with a turning point) and

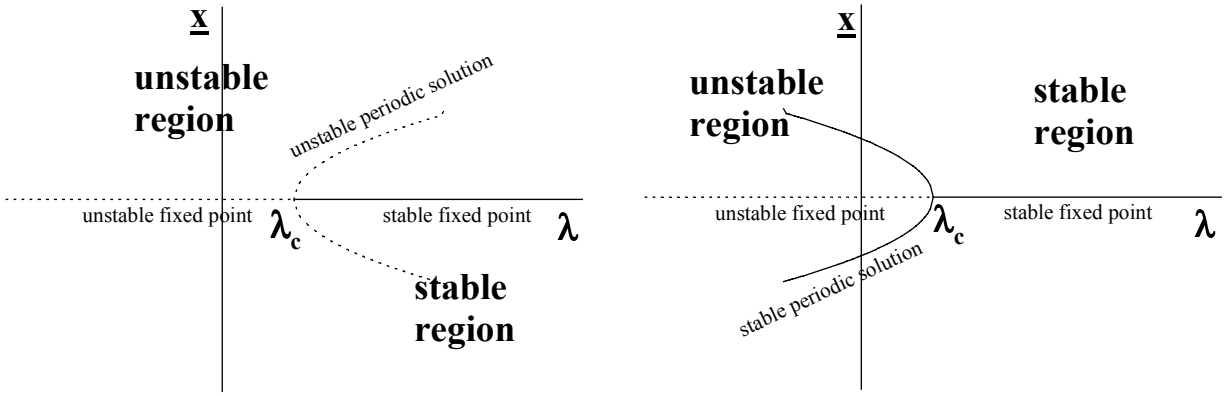

Fig. 1. Sub- and supercritical PAH bifurcations. Periodic solutions in subcritical case are unstable, and those in supercritical case are stable.

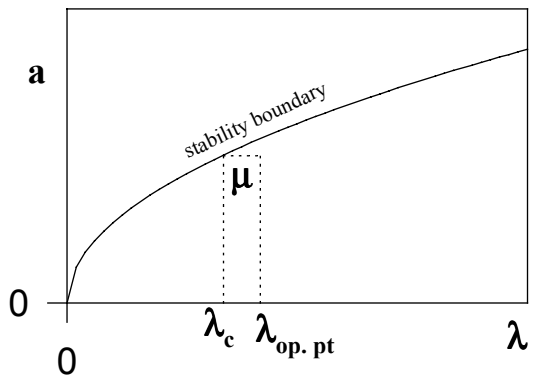

Fig. 2. Small parameter μ of the asymptotic expansion analysis in a - λ plane.

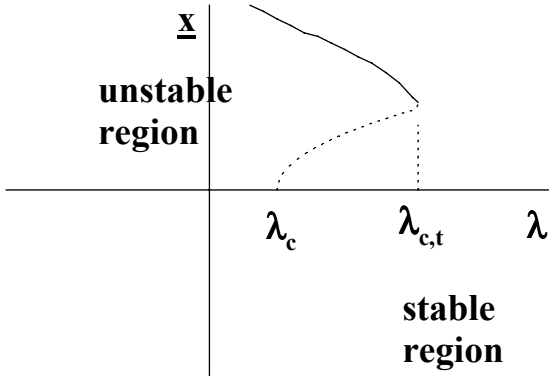

Fig. 3. Subcritical bifurcation with a turning point. Upper branch is stable.

supercritical PAH bifurcation is that the oscillation amplitude in the latter case at a point in the unstable region infinitesimally close to the stability boundary is *infinitesimally small*, while the former case leads to *large* amplitude stable oscillations (compare Figs. 1(b) and 3 for λ close to but less than λ_c). Hence, appearance in operating systems of large amplitude stable oscillations after relatively small change in parameter values suggest the possibility of subcritical PAH bifurcation coupled with a turning point (rather than supercritical PAH bifurcation). Additional scenarios in bifurcation diagrams with more than one turning points are also possible [36].

2.2 PAST WORK ON BIFURCATION ANALYSIS

The seminal bifurcation study of BWR dynamics by March-Leuba, Cacuci and Perez [29, 31] was carried out entirely numerically. Similar studies on stability of two-phase flow in heated channels (no neutronics) have also been carried out [45, 46]. Such numerical studies, being very time consuming, are restricted to small regions in parameter space. First analytical bifurcation study of two-phase flow stability without neutronics (using the homogeneous equilibrium model), was by Achard, Drew and Lahey [47]. This was later extended by Rizwan-uddin and Dorning [48], who analyzed uniformly and non-uniformly heated channels using the drift flux model to represent the two-phase flow. For *nuclear-coupled thermal hydraulic instabilities*, this approach has been used by Muñoz-Cobo and Verdú [30], Tsuji et al. [24], and by van Bragt, Rizwan-uddin and van Der Hagen [32, 33]. The drawback of the fully, "analytical" approach—like that performed by Muñoz-Cobo and Verdú [30]—is that the algebraic complexity increases rapidly with the number of equations. To avoid cumbersome algebra, Tsuji et al. [24] used a computer code called BIFOR2 [43], and showed that the bifurcation, under certain conditions, is subcritical. A successor to BIFOR2 called, BIFDD [44], was used by van Bragt, Rizwan-uddin and van Der Hagen for bifurcation analysis of nuclear-coupled thermal hydraulics in natural circulation BWRs [32, 33].

Since the BWR model used in this study is the same as that used by March-Leuba, Cacuci and Perez [29] and later used by Muñoz-Cobo and Verdú [30] in an analytical counterpart of part of that analysis, these two works are discussed in some detail here. March-Leuba, Cacuci and Perez [29] used a reduced order, 5-equation, phenomenological model to study the nonlinear dynamics of BWRs. The model was customized by fitting parameters in the model to yield the transfer function measured from operating BWRs. Authors fitted the model with a set of parameter values that lead to the transfer function corresponding to the transfer function of test 7N of the Vermont Yankee reactor. Keeping all other parameters in this model fixed and systematically varying one parameter, via *numerical integration* they showed that after the stability threshold is crossed, stable limit cycle oscillations appear followed by a cascade of period doubling bifurcations, leading to chaos. The authors chose the parameter that controls the feedback gain to be the bifurcation parameter. This parameter, represented by k, is proportional to the void reactivity coefficient and fuel heat transfer coefficient. Muñoz-Cobo and Verdú performed an *analytical* local bifurcation analysis of the same 5-equation model with k (they called it a_3) as their bifurcation parameter. The analysis results in the Poincaré normal form of the 5-equation model, and yields information regarding the nature of

bifurcation at the critical point (without numerical integration). Muñoz-Cobo and Verdú also determined the bifurcation to be supercritical and hence confirmed the results obtained in Ref. 29.

Tsuji et al. [24] on the other hand, using a different BWR model operating under operating conditions different from those studied in Ref. 29 and 30 found the nature of bifurcation to be subcritical. Karve, Rizwan-uddin and Dorning [27] also determined the bifurcation in a model they developed for out-of-phase oscillations in BWRs to be subcritical. Since the studies that predicted supercritical PAH bifurcation and those that predicted subcritical PAH bifurcations used different NCTH models, it is not straightforward by comparing these studies to determine the parametric dependence of bifurcation. Within the context of a single model, researchers have usually restricted their bifurcation studies to a narrow region of the parameter space, and hence have reported either sub- or supercritical PAH bifurcations. Therefore, to resolve the issue of the parametric dependence, relatively large regions of the parameter space of a BWR model must be explored.

3. MODEL

The phenomenological model of BWR used in Ref. 29 and 30 is given by

$$\frac{dn(t)}{dt} = \frac{\rho(t) - \beta}{\Lambda} n(t) + \lambda c(t) + \frac{\rho}{\Lambda} \tag{12}$$

$$\frac{dc(t)}{dt} = \frac{\beta}{\Lambda} n(t) - \lambda c(t) \tag{13}$$

$$\frac{dT(t)}{dt} = a_1 n(t) - a_2 T(t) \tag{14}$$

$$\frac{d^2 \rho_\alpha(t)}{dt^2} + a_3 \frac{d\rho_\alpha(t)}{dt} + a_4 \rho_\alpha(t) = k T(t) \tag{15}$$

where $\rho(t) = \rho_\alpha(t) + DT(t)$, and each phase variable represents deviation relative to its steady-state value. Hence, $n(t) = (N(t) - N_0)/N_0$, etc. [29]. Replacing Eq. (15) by

$$\frac{d\rho_\alpha(t)}{dt} = \rho_t(t) \tag{16}$$

$$\frac{d\rho_t(t)}{dt} = -a_3 \rho_t(t) - a_4 \rho_\alpha(t) + k T(t) \tag{17}$$

yields the set of five, nonlinear, first order ordinary differential equations (Eqs. 12-14, 16 and 17).

The vector of unknown phase variables $[n, c, T, \rho_\alpha, \rho_t]^T$ will be represented by $\underline{x(t)}$, and the vector of parameters is divided up into two groups, $\underline{\mu_1} = [k, a_1, a_2, a_3, a_4, D]^T$, and $\underline{\mu_2} = [\beta, \Lambda, \lambda]^T$. Full-power operating (fixed) point corresponds to $\underline{x} = [0,0,0,0,0]^T$. Jacobian of the above set of equations can be easily evaluated.

A subroutine is written in FORTRAN to numerically evaluate the right hand side of the set of nonlinear ODEs as well as its Jacobian. Subroutine BIFDD calls this subroutine as needed. A main program is written that allows selection of any one of the nine parameters as the bifurcation parameter. It also allows the selection of a second parameter, which is to be incremented in small steps allowing repeated evaluation of the critical value of the bifurcation parameter. Any of the remaining eight parameters can be selected as the *second* (incremented) parameter. Numerical integration of the dynamical system was carried out using WINPP, a dynamical system analysis program for personal computers [49].

4. RESULTS

4.1 ANALYTIC-NUMERIC BIFURCATION STUDIES

The program BIFDD, for each value of the incremented parameter, calculates the critical value of the bifurcation parameter (point on the stability boundary), frequency corresponding to the critical value, and expansion parameters μ_2, τ_2, and β_2. Using Eq. (8), the program also calculates the value of the bifurcation parameter at which the oscillation amplitude will have a user-specified value ε.

Unless explicitly stated otherwise, set of parameters originally used by March-Leuba, Cacuci and Perez [29] are used. These are: $\underline{\mu_1} = [k, 25.04, 0.23, 2.25, 6.82, -2.52e\text{-}5]^T$ and $\underline{\mu_2} = [0.0056, 4.0e\text{-}5, 0.08]^T$. For these parameter values and k as the bifurcation parameter, the critical value of k is determined to be -3.7036e-3 (K^{-1}-s^{-2}), which compares very well with the value of -3.7e-3 reported in Ref. 29.

Stability and bifurcation analyses were then systematically performed choosing different bifurcation parameters. In figures that present results in 2-D parameter spaces, the parameter on the horizontal axis was the bifurcation parameter while the parameter on the vertical axis was incremented in small steps. Shown are the stability boundaries and the results of the bifurcation analysis. Constant amplitude oscillation curves are plotted for oscillation amplitude of 5, 10 and 15% (of the steady-state value). These curves represent supercritical PAH bifurcation when they are on the unstable side of the stability boundary, and subcritical PAH bifurcation when on the stable side.

Figure 4(a) shows the stability boundary in the $a_3 - k$ plane. Corresponding bifurcation diagram in $a_3 - (k - k_c)$ plane (Fig. 4(b)) shows that for $0 < a_3 < 0.40$ and $5.2 < a_3 < 6$, subcritical PAH bifurcation is predicted. Supercritical PAH bifurcation is predicted for $0.4 < a_3 < 5.2$. Similar results are presented in Figs. 5 through 15 in other two-dimensional parameter spaces. Parameter k is set equal to –0.0037 in Figures 8, 9 and 11 through 15. In some cases, such as in Fig. 10, only super-

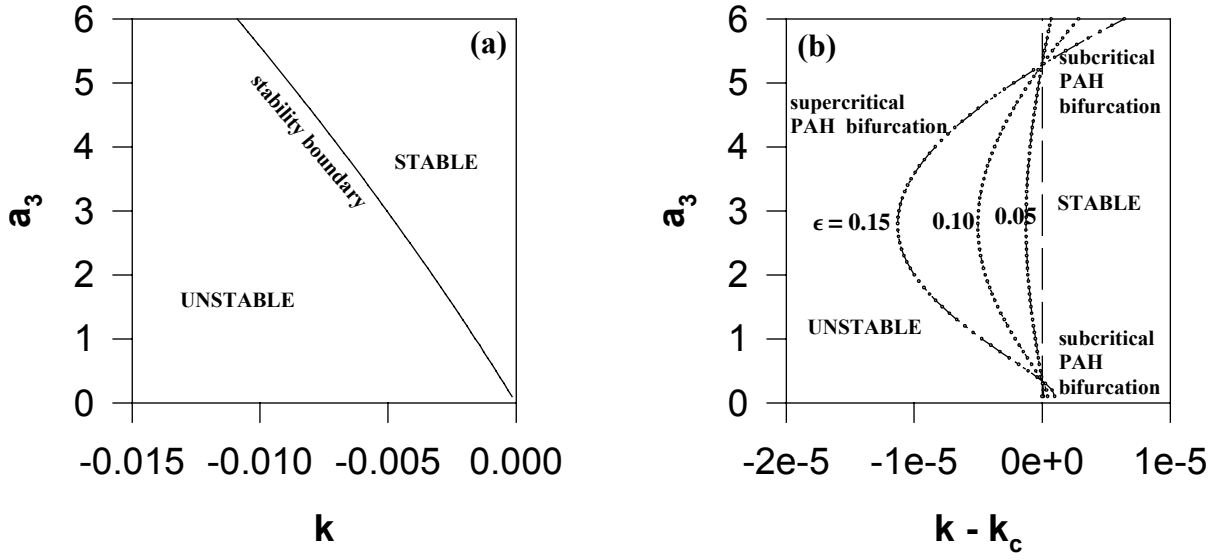

Fig. 4. Stability boundary in a_3 - k plane and results of the bifurcation analysis in a_3 - $(k-k_c)$ plane. $(k - k_c) = 0$ is the stability boundary.

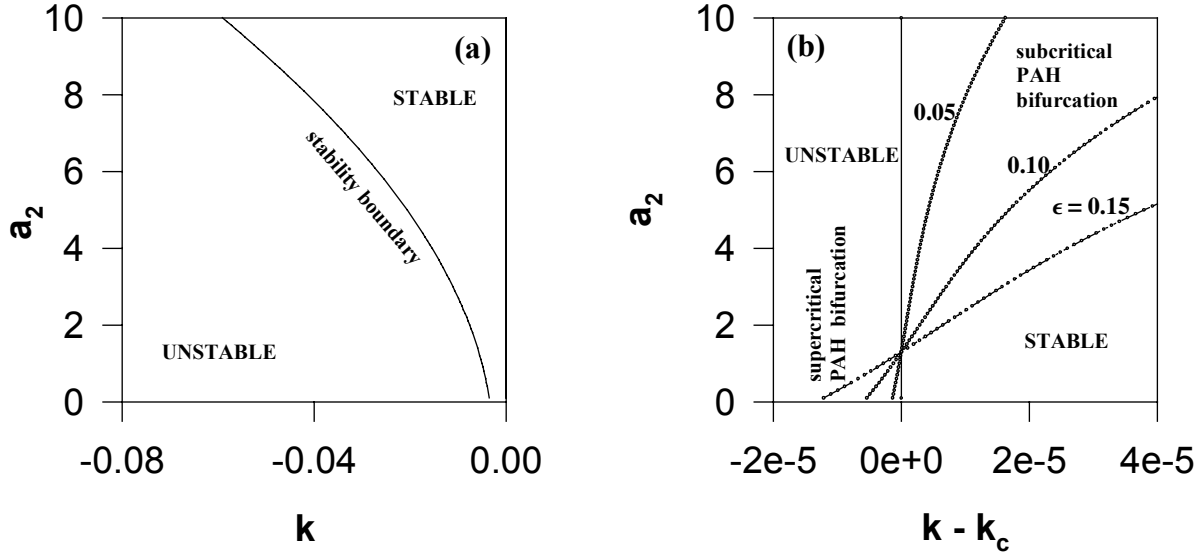

Fig. 5. Stability boundary in a_2 - k plane and results of the bifurcation analysis in a_2 - $(k-k_c)$ plane. $(k - k_c) = 0$ is the stability boundary.

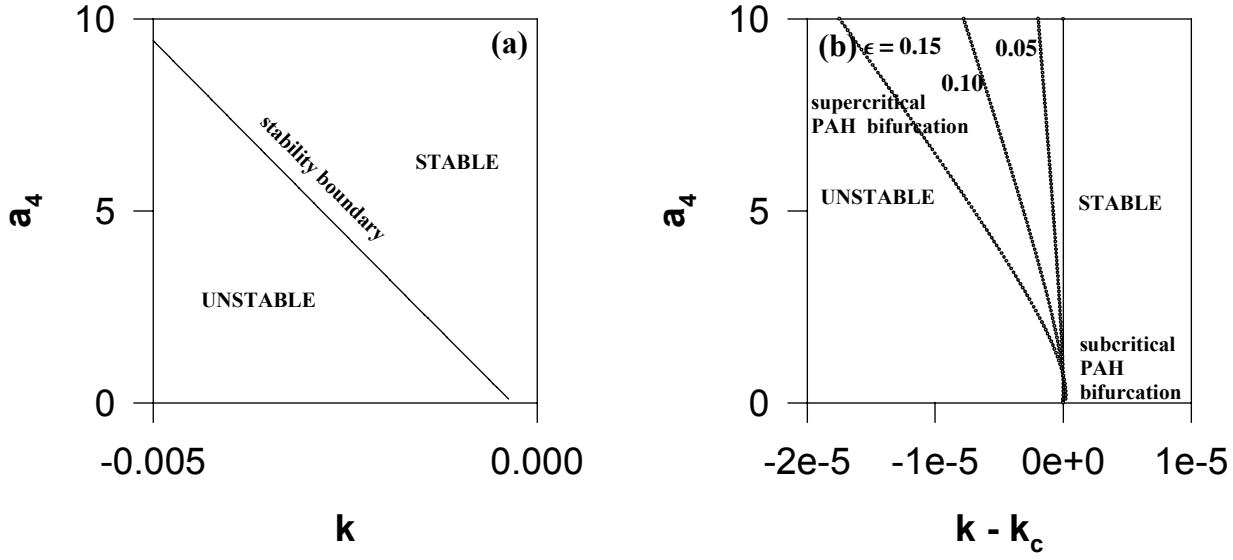

Fig. 6. Stability boundary in a_4 - k plane and results of the bifurcation analysis in a_4 - $(k-k_c)$ plane. $(k - k_c) = 0$ is the stability boundary.

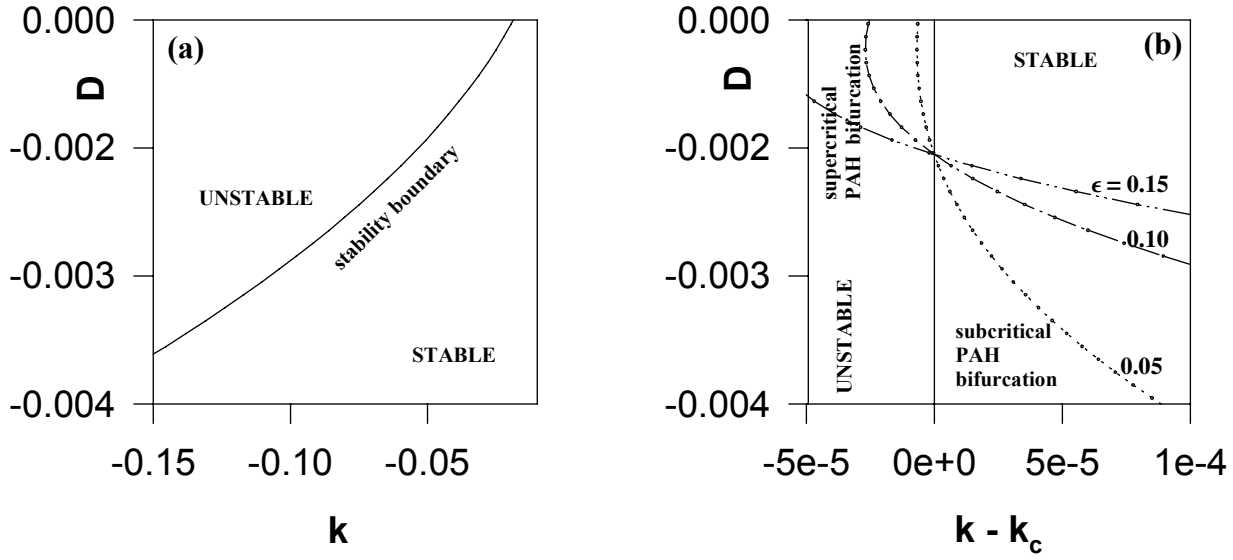

Fig. 7. Stability boundary in D - k plane and results of the bifurcation analysis in D - $(k-k_c)$ plane. $(k - k_c) = 0$ is the stability boundary.

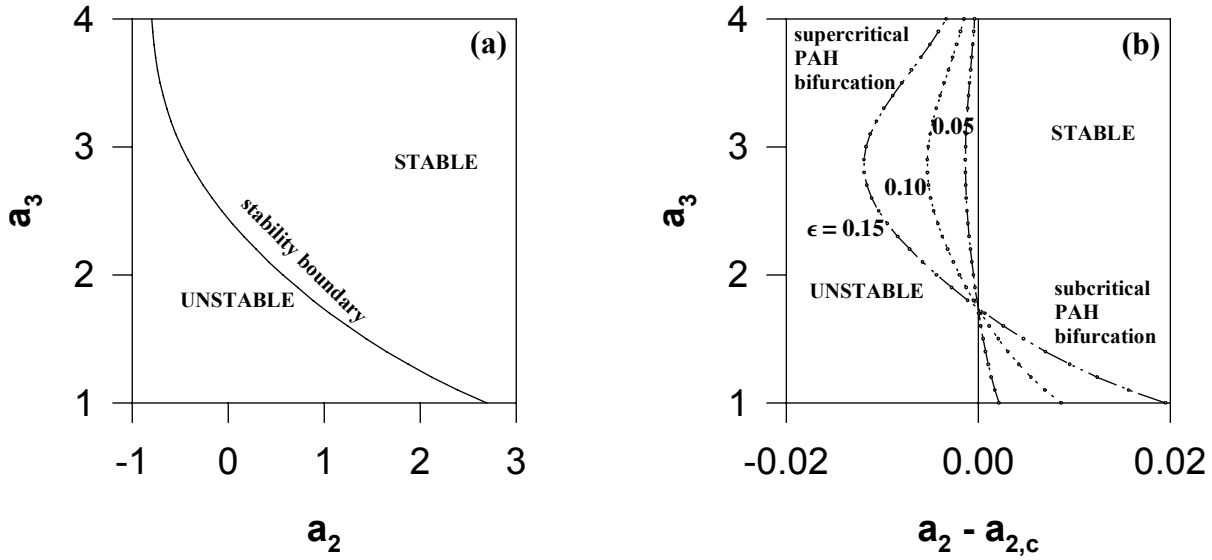

Fig. 8. Stability boundary in a_3 - a_2 plane and results of the bifurcation analysis in a_3 - $(a_2 - a_{2,c})$ plane. $(a_2 - a_{2,c}) = 0$ is the stability boundary.

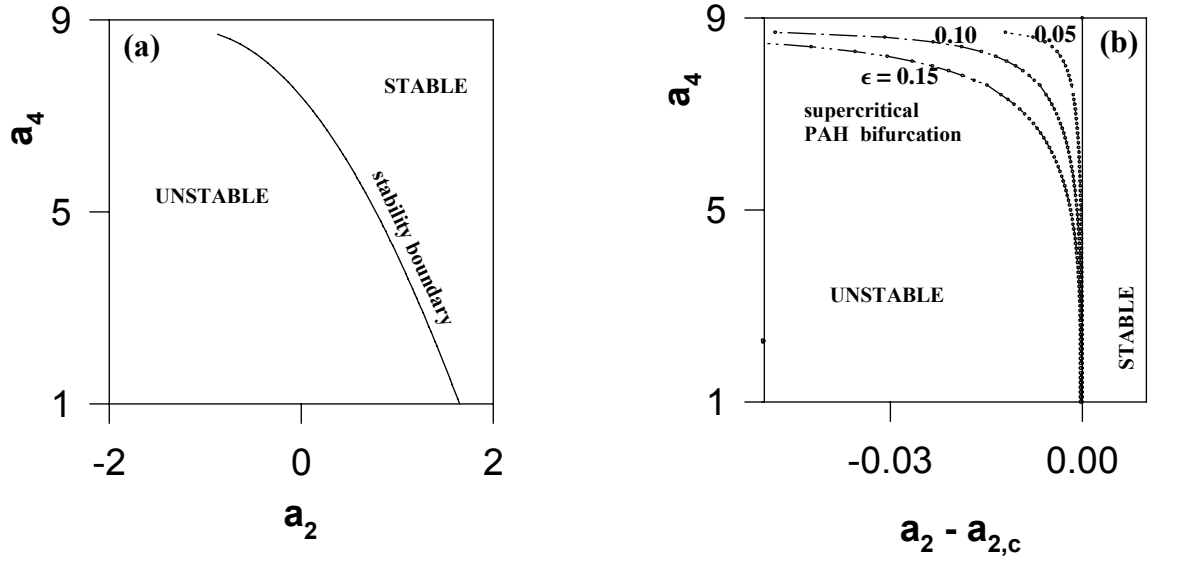

Fig. 9. Stability boundary in a_4 - a_2 plane and results of the bifurcation analysis in a_4 - $(a_2 - a_{2,c})$ plane. $(a_2 - a_{2,c}) = 0$ is the stability boundary.

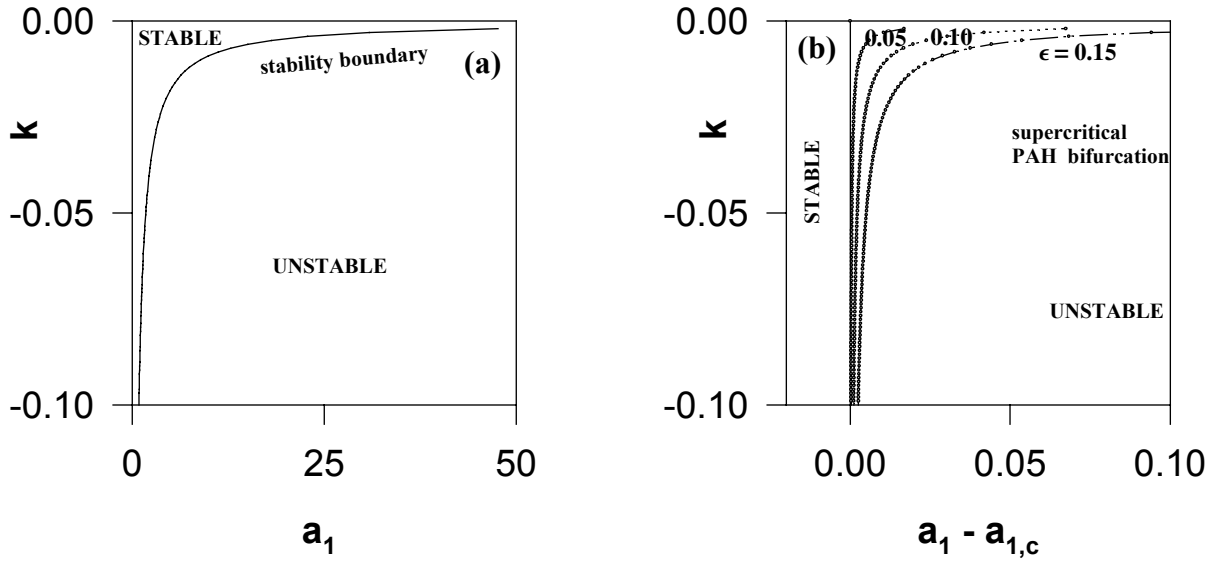

Fig. 10. Stability boundary in k - a_1 plane and results of the bifurcation analysis in k - $(a_1 - a_{1,c})$ plane. $(a_1 - a_{1,c}) = 0$ is the stability boundary.

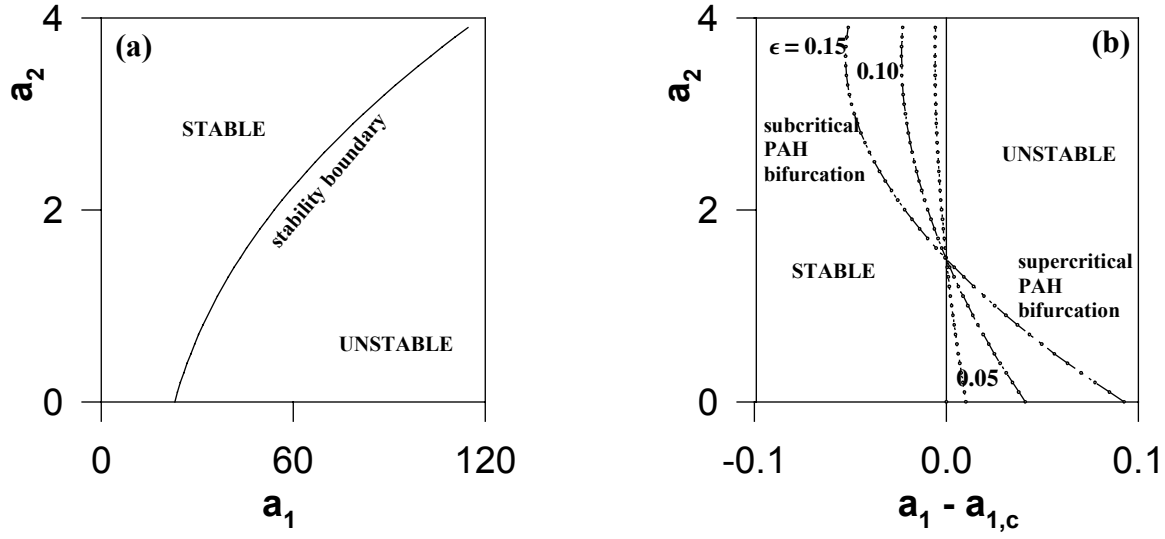

Fig. 11. Stability boundary in a_2 - a_1 plane and results of the bifurcation analysis in a_2 - $(a_1 - a_{1,c})$ plane. $(a_1 - a_{1,c}) = 0$ is the stability boundary.

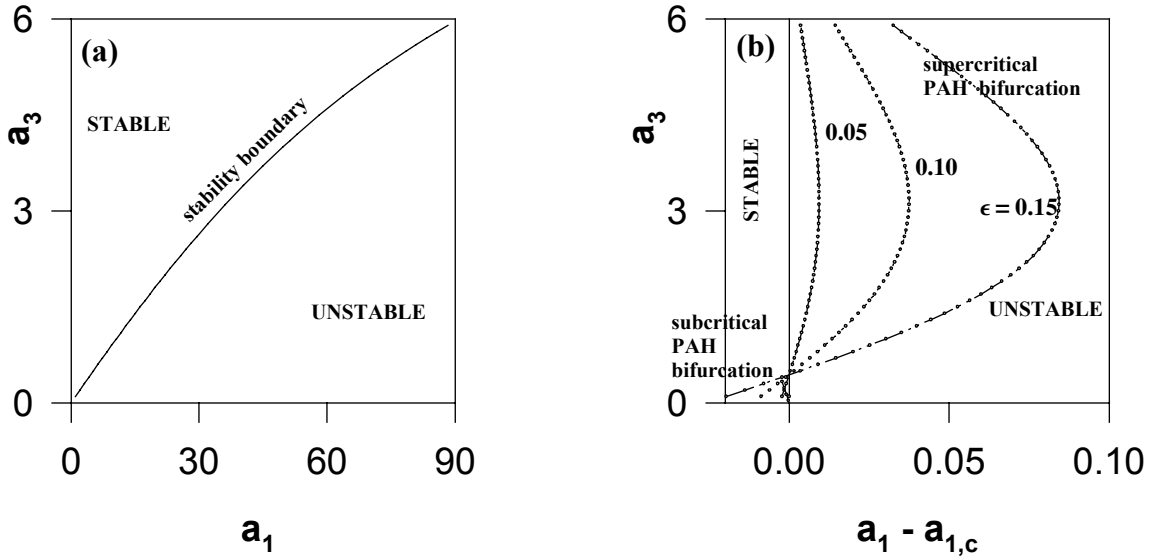

Fig. 12. Stability boundary in a_3 - a_1 plane and results of the bifurcation analysis in a_3 - $(a_1 - a_{1,c})$ plane. $(a_1 - a_{1,c}) = 0$ is the stability boundary.

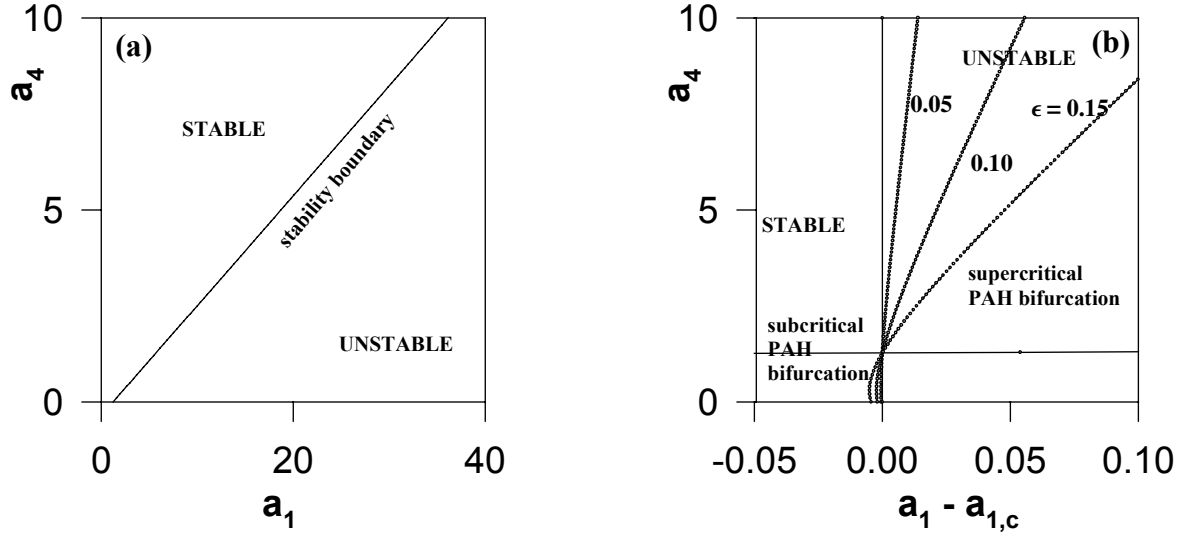

Fig. 13. Stability boundary in a_4 - a_1 plane and results of the bifurcation analysis in a_4 - $(a_1 - a_{1,c})$ plane. $(a_1 - a_{1,c}) = 0$ is the stability boundary.

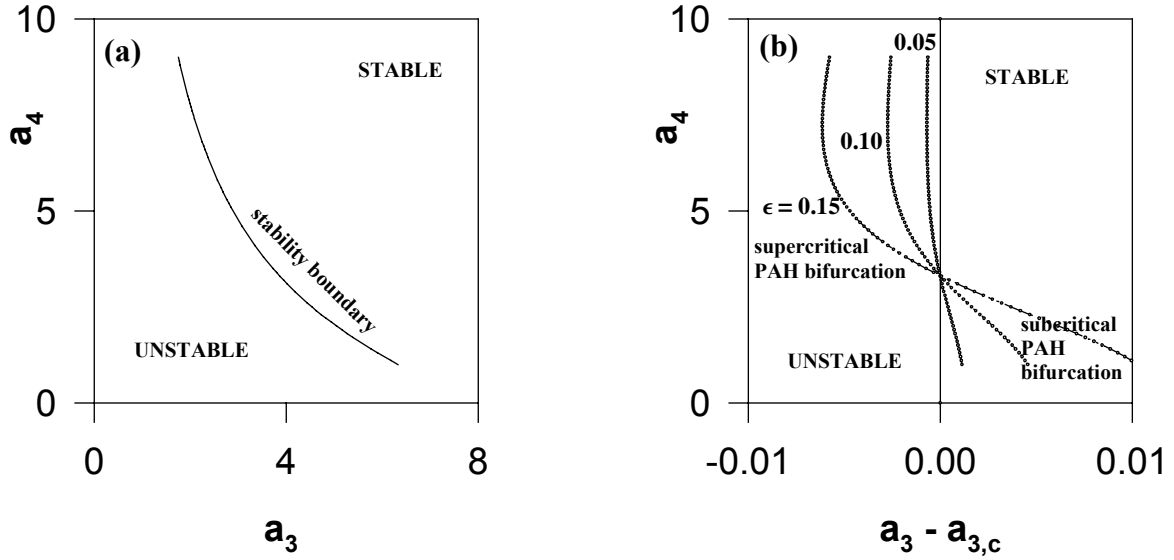

Fig. 14. Stability boundary in a_4 - a_3 plane and results of the bifurcation analysis in a_4 - $(a_3 - a_{3,c})$ plane. $(a_3 - a_{3,c}) = 0$ is the stability boundary.

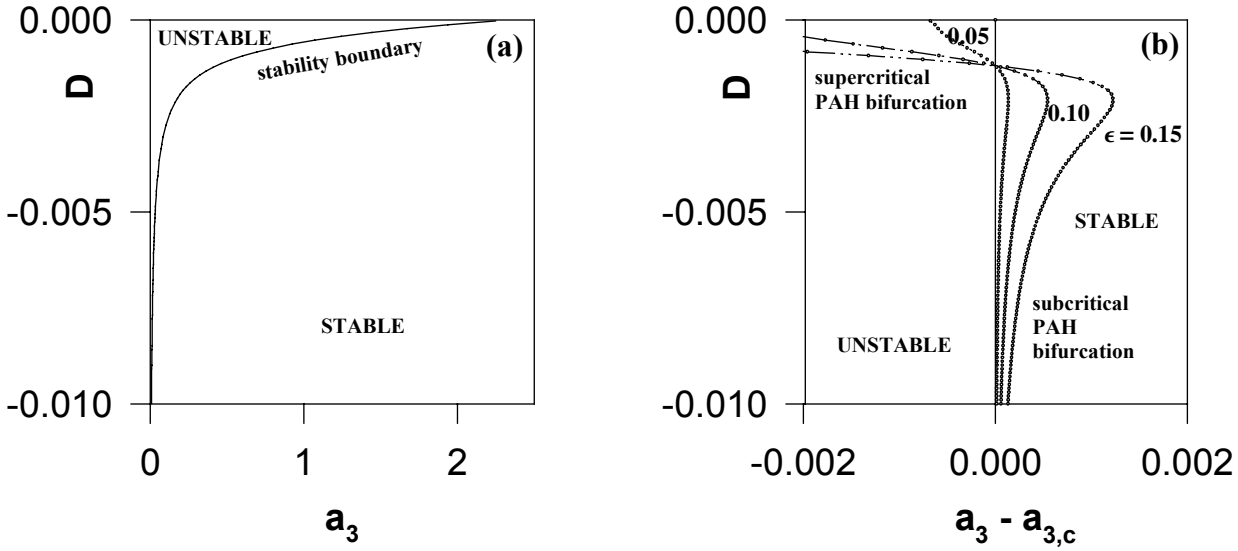

Fig. 15. Stability boundary in D - a_3 plane and results of the bifurcation analysis in D - $(a_3 - a_{3,c})$ plane. $(a_3 - a_{3,c}) = 0$ is the stability boundary.

critical PAH bifurcation is found over the range of parameter values studied. Results presented in Fig. 10(a) are actually trivial since it is known that the stability boundary in $a_1 - k$ plane is given by $a_1 k = constant$. However, growth in oscillation amplitude as the operating point is moved away from the stability boundary depends upon particular combination of a_1 and k. Amplitude, as shown in Fig. 10(b), increases much faster with a_1 for lower values of k than it does for larger values of k.

Past studies, being restricted to only one set of values for all parameters other than the bifurcation parameter, only reported a single critical (bifurcation) value of the bifurcation parameter, and consequently only one kind of bifurcation (sub- or supercritical) was found. In the present study, determination of the critical value of the bifurcation parameter as a second parameter is incremented has allowed to unfold the bifurcation point (critical value) in a second dimension, allowing both kinds of bifurcations to be determined and presented in two-dimensional parameter spaces. Results presented here clearly show the parametric dependence of the nature of bifurcation. For example, bifurcation changes from supercritical to subcritical as the absolute value of D (Doppler feedback) is increased (Figs. 7 and 15).

It should be remembered that the model used here only allows qualitative conclusions to be drawn. However, if the reduced order model is qualitatively faithful to the nonlinear aspects of the system it is intended to simulate, the *real* transition points between sub- and supercritical bifurcations in parameter space are expected to be inside a strip centered at the transition point as determined using the reduced order model.

4.2 NUMERICAL STUDIES

The set of five nonlinear ODEs (Eqs. 12-14, 16 and 17) are integrated numerically using the GEAR algorithm to determine the system behavior at parameter values away from the stability boundaries, and for the effect of perturbation amplitude on the final state to which the system evolves. Figures 16(a) through 16(c) show some typical evolution of the normalized neutron number density, $n(t)$. In each case the initial condition is, $\underline{x}(t=0) = [1, 1, 1, 0, 0]^T$. The sequence of period doubling bifurcation leading to chaos first reported in Ref. 29 was also reproduced.

Numerical integrations were carried out for several sets of parameter values. Results for three of these corresponding to Figures 4, 6 and 12 are presented here. For $a_3 = 5.5$, Fig. 4 shows that bifurcation analysis predicts a subcritical PAH bifurcation. Critical value of $k = k_c = -0.009859$. Also, $k > k_c$ is stable and $k < k_c$ is unstable. Results reported here were obtained with $\underline{x}(t = 0) = [5, 5, 0.1, 0, 0]^T$ for the small perturbation case, and $\underline{x}(t = 0) = [100, 10, 0.1, 0, 0]^T$ for the large perturbation case. Figure 17 shows the evolution of the neutron number density for two different sets of initial conditions (same parameter values). k for both cases is $-0.00983 (> k_c)$. Hence, the operating point is in the stable region. Results of the numerical integration with small perturbation, Fig. 17(a), confirm the findings of the BIFDD results. Here, the initial condition—being in the basin of attraction of the stable fixed point—decays, though very slowly, to the fixed point. Moreover, as shown in Fig. 17(b), when the initial condition is outside the basin of attraction of the stable fixed

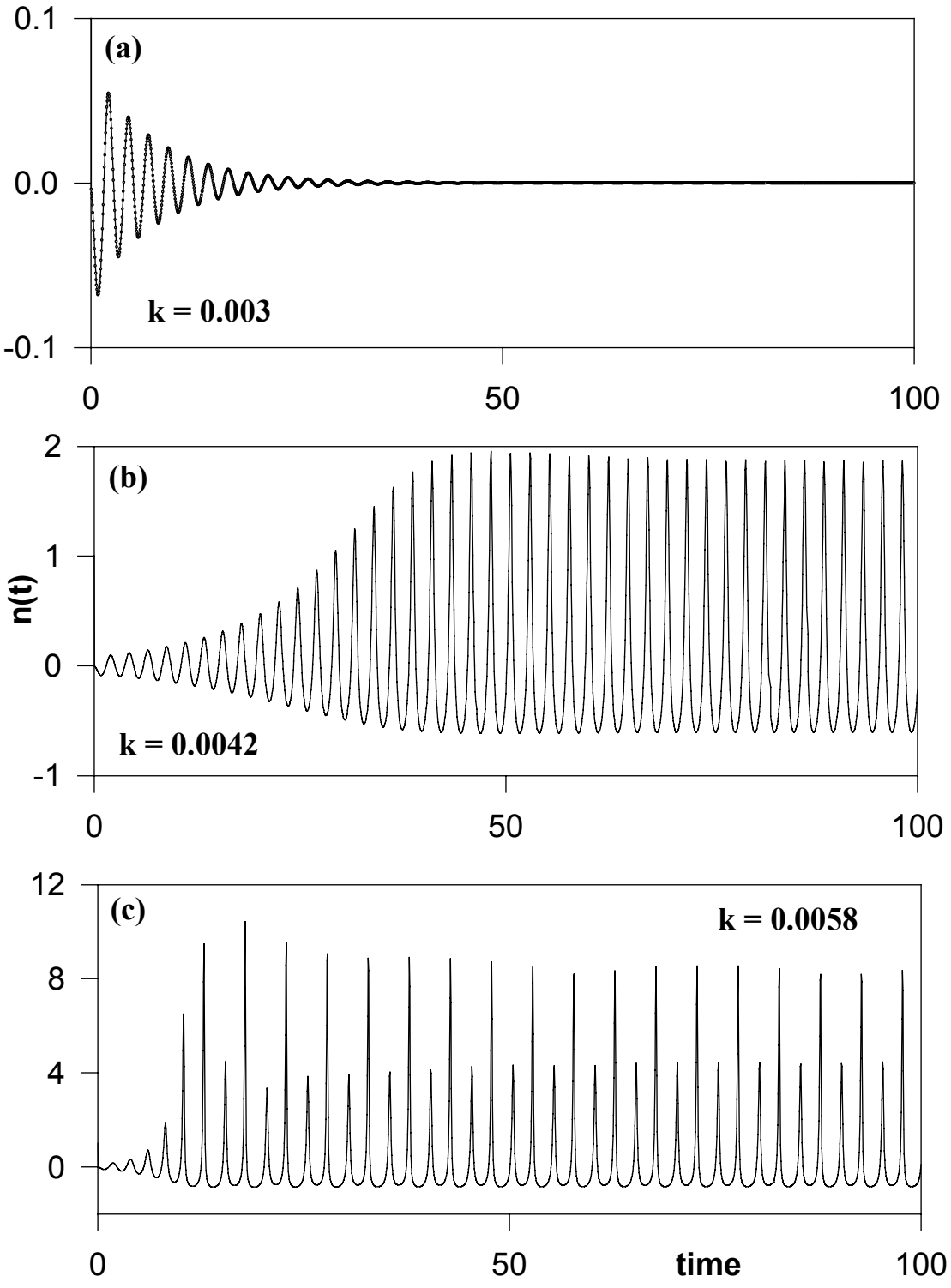

Fig. 16. Three typical evolutions of the excess neutron number density.

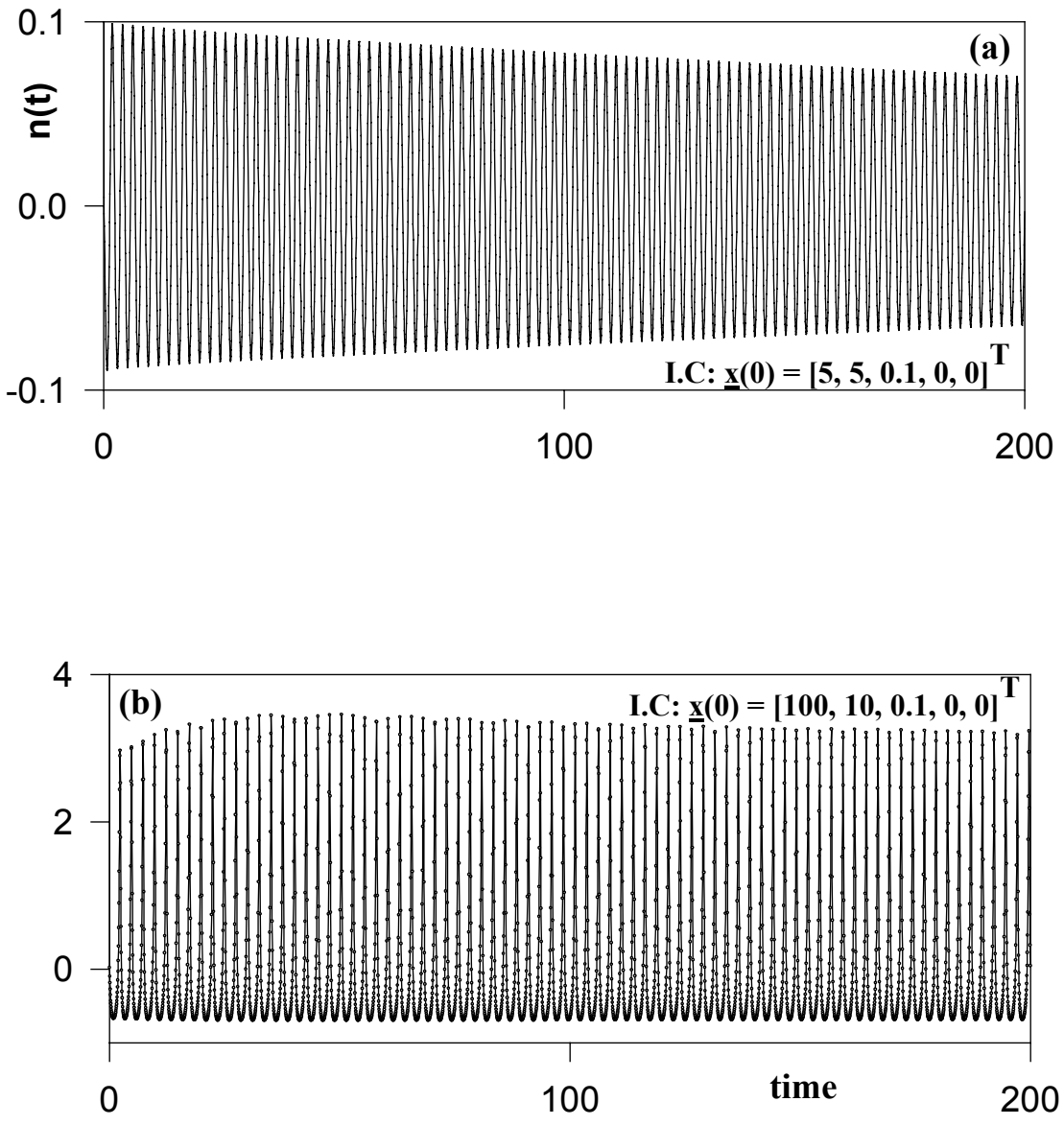

Fig. 17. Subcritical bifurcation case. a) Small amplitude perturbation decays to the stable fixed point. b) Large amplitude perturbation evolves to the stable limit cycle. k and a_3 for both cases are -0.00983 and 5.5, respectively.

point, the system evolves to a large amplitude stable limit cycle (with oscillation amplitude of about 3.2), suggesting that there is a turning point in the bifurcation diagram. Further numerical integrations show that the turning point occurs at a k value that lies between *–0.00982* and *–0.00981*. Evolution for k slightly less that the critical value ($k = -0.01 < k_c = -0.009859$), even when starting from a very small perturbation, shows the existence of a large amplitude stable limit cycle with oscillation amplitude of approximately ~6.8, suggesting that the *turned-around* bifurcation curve continues into the unstable region. Numerically determined bifurcation diagram is shown in Fig. 18. Not shown in Fig. 18 is the data point corresponding to $k = -0.011$ which leads to stable oscillations with an amplitude of about 19.

A similar sequence of numerical integrations for several values of k shows that for $a_4 = 5$ (supercritical case, Fig. 6) there is a sequence of period doubling bifurcations similar to that found for $a_4 = 6.25$.in Ref. 29. However, for $a_4 = 0.6$ (subcritical case, Fig. 6) there is a turning point in the bifurcation diagram similar to that shown in Fig. 18 (k being the bifurcation parameter) that lies between *0.0060* and *0.0065*.

Analytically predicted oscillation amplitudes are compared with the numerical predictions in Fig. 19. Plotted are analytically predicted oscillation amplitude for three different values of a_3 ($a_3 = 1.0, 3.0$ and *5.5* in Fig. 12*)* as a function of distance from the stability boundary (into the unstable region). Also shown are curves with data symbols on them (connected by straight lines) that represent oscillation amplitude predicted by numerical integrations. Oscillation amplitude for numerical simulations is defined as the average of the absolute values of n_{max} and n_{min} over a cycle where n is the excess neutron number density. It is interesting to note that analytically predicted oscillation amplitude continues to agree fairly well with the numerically determined oscillation amplitude even when the stable limit cycles cease to be sinusoidal. For example, for $a_3 = 3.0$ and $a_1 - a_{1,c} = 1.21$, the limit cycle oscillations are similar to those shown in Fig. 16(b), i.e., fairly asymmetric about the nominal value of neutron density. However, despite this asymmetric limit cycle, the analytical prediction of ~0.57 for the amplitude of the (symmetric) limit cycle agrees fairly well with the value of ~0.6 predicted by numerical integration. Numerical results further show that, as predicted by the bifurcation analysis (Fig. 12), the oscillation amplitude rises faster as a function of a_1 for $a_3 = 1.0$ and *5.5* than it does for $a_3 = 3.0$.

SUMMARY AND CONCLUSIONS

Taking advantage of general purpose codes for analytic-numeric bifurcation, and those developed to efficiently perform numerical integrations on PCs, qualitative BWR dynamics has been studied using a simple phenomenological model. Stability boundaries are obtained in several two-dimensional parameter spaces. Results of the bifurcation analysis along these stability boundaries clearly show that there are regions in parameter space where the model predicts subcritical PAH bifurcation and other regions where supercritical PAH bifurcation is predicted. These results are confirmed by numerical integration of the set of ODEs.

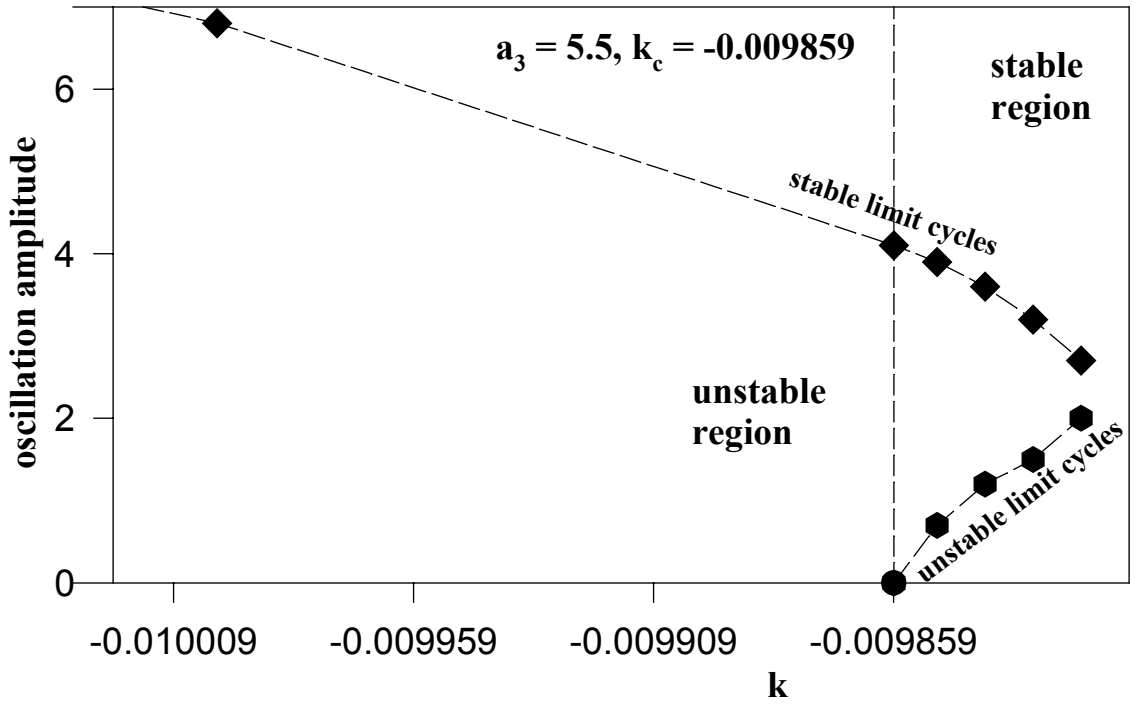

Fig. 18. Bifurcation diagram for subcritical case with a turning point. Lower branch is schematic. Data points on the upper branch are calculated by numerically integrating the governing equations.

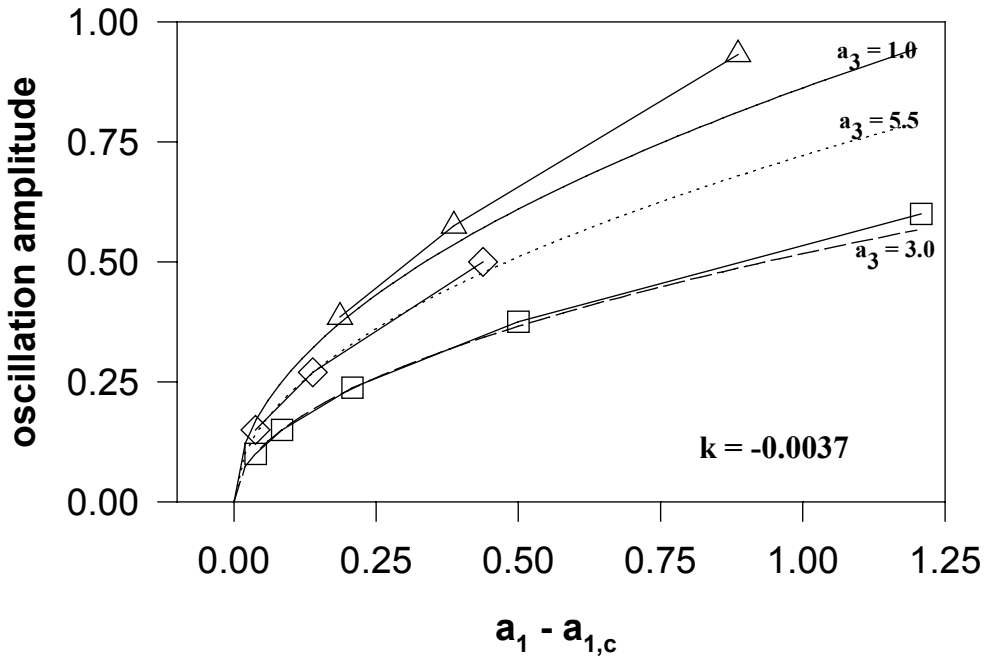

Fig. 19. Oscillation amplitude as a function of distance from the stability boundary. Curves without symbols are analytical predictions. Curves with symbols are discrete data points determined numerically.

Numerical integrations further show that bifurcation diagrams in most cases of subcritical PAH bifurcation have a turning point, thus implying that growing amplitude oscillations in the subcritical strip adjacent to the stability boundary are nevertheless bounded.

Operational parameters in the model used (at least k, a_1, a_2 and D) have direct physical significance, and hence results presented in Figs. 4-15 can be used to deduce parametric dependence of bifurcation on these physically relevant parameters. However, *physical* explanation of transition from sub- to supercritical bifurcation (or vice versa) as a physical parameter is changed remains a challenge.

REFERENCES

1. J. March-Leuba and J.M. Rey, "Coupled Thermohydraulic-Neutronic Instabilities in Boiling Water Nuclear Reactors: A Review of the State of the Art," *Nucl. Eng. Des*., **145**, 99 (1993).

2. Proceedings of the International Workshop on Boiling Water Reactor Stability, Sponsored by the Nuclear Energy Agency of the Organization for Economic Cooperation and Development, OECD-NEA, CSNI Report 178, Brookhaven, NY, October, 1990.

3. Rizwan-uddin, "Two-Phase Density-Wave Oscillations and Nuclear-Coupled Two-Phase Thermal Hydraulic Instabilities: A Review," in the Proc. of the first ISHMT-ASME Heat and Mass Transfer Conference, pp. 511-520, Bombay, India, January 5-7, 1994.

4. Y.M. Farawila, D.W. Pruitt and P.E. Smith, "Analysis of the Laguna Verde Instability Event," ANS Proc., 1996 National Heat Transfer Conf., HTC-Vol. 9, pp. 198-202, Am. Nucl. Soc., La Grange Park, IL, 1996.

5. M. Kruners, "Analysis of Instability Event in Oskarshamn-3, Feb. 8, 1998, with Simulate-3K," SKI Rapport, 98:42, ISSN 1104-1374, December 1998.

6. J. March-Leuba and E.D. Blakeman, "A Mechanism for Out-of-Phase Power Instabilities in Boiling Water Reactors," *Nucl. Sci. Eng*., **107**, 173 (1991).

7. B.G. Bergdahl, F. Reisch, R. Oguma, J. Lorenzen and F. Akerhielm, "BWR Stability Investigation at Forsmark-1," *Ann. Nucl. Energy* **16**, No. 10, 509-520 (1989).

8. E. Gialdi, S. Grifoni, C. Parmeggiani and C. Tricoli, "Core Stability in Operating BWR: Operational Experience," *Progress in Nuclear Energy*, **15**, 447-459 (1985).

9. H.S. Cheng, J.G. Guppy, A.N. Mallen and W. Wulff, "Simulations of the Recent LaSalle-2 Incident with BNL Plant Analyzer," *Trans. Amer. Nucl. Soc*., **57**, 385 (1988). Also see: "Reactor Scram on High Average Power Range Monitor Flux Level Due to Personnel Valving Error," LER 88-003-00, Commonwealth Edison Company (April 7, 1988); G.A. Murphy, "Power Oscillations at LaSalle 2," *Nuclear Safety*, **29**, 356 (1988).

10. W. Wulff, H.S. Cheng, A.N. Mallen and U.S. Rohatgi, "BWR Stability Analysis with the BNL Engineering Plant Analyzer," BNL-NUREG-52312 (1992).

11. W. Wulff, "A Description and Assessment of RAMONA-3B MOD0 cycle 4: A Computer Code with Three Dimensional Neutron Kinetics for BWR System Transients," NUREG/CR-3664, 1984.

12. F.D. Giust and L. Moberg, "RAMONA Stability Analysis on Ringhals-1, Phase 1: Model

Qualification," TR1/42.83.06, ScandPower (1991). Also see: G.M. Grandi and F.D. Giust, "RAMONA Stability Analysis on Ringhals-1, Phase 2: Predictive Calculations," TR2/42.83.06, ScandPower (1991).

13. A. Hotta, H. Ninokata and A. Baratta, "Development of Three Dimensional Kinetic Code ENTREE Coupled with TRAC-BF1," Proc. Nuclear Reactor Thermal Hydraulics Conference, NURETH-9, CD, American Nuclear Society (1999).

14. K. Valtonnen, "RAMONA-3B and TRAB Assessment Using Oscillation Data from TVO-I," Proc. Int. Workshop on BWR Stability, OECD-NEA, CSNI Report 178, 205-231, 1990.

15. J. C. Shaug, J.G.M. Andersen, and J.K. Garrett, "TRACG Analysis of BWR Plant Stability Data," *Proc. Int. Workshop on BWR Stability*, OECD-NEA CSNI Report 178, 55 (1990).

16. F. Araya, M. Hirano, K. Yoshida, K. Matsumoto, M. Yokobayashi, and A. Kohsaka, "Summary of RETRAN Calculations on LaSalle 2 Neutron Flux Oscillation Event Performed at JAERI," *Proc. Int. Workshop on BWR Stability*, OECD-NEA CSNI Report 178, 370 (1990).

17. Y. Takigawa, Y. Takeuchi, S. Tsunoyama, S. Ebata, K.C. Chan, and C. Tricoli, "Coarso Limit Cycle Oscillation Analysis With Three-Dimensional Transient Code TOSDYN-2," *Nucl. Technol.*, **79**, 210 (1987).

18. Y. Takeuchi,Y. Takigawa, S. Tsunoyama and A. Kojima, "Analysis of Selected Rod Insertion Test in BWR Plant with Three Dimensional Transient Code TOSDYN-2," *J. Nucl. Sci. Tech.*, **28**, 3, 199-207 (1991).

19. C.J. Jackson. D.G. Cacuci, H. Finnemann, "Dimensionally Adaptive Neutron Kinetics for Multidimensional Reactor Safety Transients—I: New Features of RELAP5/PANBOX," *Nucl. Sci. Eng.*, **131**, 143 (1999). And II: Dimensionally Adaptive Switching Algorithms," *Nucl. Sci. Eng.*, **131**, 164 (1999).

20. D. Barber, R. Miller, H. Joo, T. Downar, W. Wang, V. Mousseau and D. Ebert, "Coupled 3-D Reactor Kinetics and Thermal Hydraulic Code Activities at the US Nuclear Regulatory Commission," in the Proc. *M&C'99—International Conference on Mathematics and Computation, Reactor Physics and Environmental Analysis in Nuclear Applications*, Madrid, Spain, p. 311-320, September, 27-30, 1999.

21. P. Otaduy and J. March-Leuba, "LAPUR User's Guide," NUREG/CR-5421, 1989. Also see: J. March-Leuba and P. Otaduy, "A Comparison of BWR Stability Measurements with Calculations Using the Code LAPUR-IV," NUREG/CR-2998, ORNL/TM-8546, ORNL, January, 1993.

22. S.J. Peng, M.Z. Podowski, R.T. Lahey and M. Becker, "NUFREQ-NP: A Computer Code for the Stability Analysis of Boiling Water Nuclear Reactors," *Nucl. Sci. Eng*. **88**, 404-411 (1984).

23. P. Hanggi, T. Smed and P. Lansaker, "MATSTAB, A Fast Frequency Domain Based Code to Predict Boiling Water Reactor Reactor Stability Using a Detailed Three-Dimensional Model," Proc. Nuclear Reactor Thermal Hydraulics Conference, NURETH-9, CD, American Nuclear Society (1999).

24. M. Tsuji, K. Nishio and M. Narita, "Stability Analysis of BWRs using Bifurcation Theory," *J. Nuc. Sci. and Tech*., **30,** 11, 1107-1119 (1993).

25. Atul A. Karve, Rizwan-uddin and J. Dorning, "Stability Analysis of Nuclear-Coupled Thermalhydraulics in a BWR Using a Simple Model," *Nuclear Engineering & Design*, **177**, No. 1-3, 155-177 (1997).

26. A.A. Karve, Rizwan-uddin, and J.J. Dorning, "Stability Boundaries of BWRs in Operating Parameter Space and in the Power-Flow Plane," *Trans. Am. Nucl. Soc*., **75**, 392-394 (1996).

27. Atul A. Karve, Rizwan-uddin and J. Dorning, "Out of Phase Power Oscillations in Boiling Water Reactors," in the *Proc. of the Joint Int. Conf. on Mathematical Methods and Super-Computing* (held at Saratoga Springs, NY, October, 5-9, 1997), Vol. 2, pp. 1633-1647, American Nuclear Society, La Grange Park, IL, 1997.

28. D.D.B. van Bragt and T.H.J.J. van Der Hagen, "Stability of Natural Circulation Boiling Water Reactors: Part I - Description Stability Model and Theoretical Analysis in Terms of Dimensionless Groups," *Nucl. Technol.*, **121**, 40 (1998). Also see: D.D.B. van Bragt and T.H.J.J. van Der Hagen, "Stability of Natural Circulation Boiling Water Reactors: Part II - Parametric Study of Coupled Neutronic-Thermohydraulic Stability," *Nucl. Technol.*, **121**, 52 (1998).

29. J. March-Leuba, D.G. Cacuci and R.B. Perez , "Nonlinear Dynamics and Stability of Boiling Water Reactors: Part I-Qualitative Analysis," *Nucl. Sci. Eng*. **93**, 111-123 (1986).

30. J.L. Muñoz-Cobo and G. Verdú, "Application of Hopf Bifurcation Theory and Variational Methods to the Study of Limit Cycles in Boiling Water Reactors," *Ann. Nucl. Energy*, **18**, No. 5, 269 (1991).

31. J. March-Leuba, D.G. Cacuci and R.B. Perez, "Nonlinear Dynamics and Stability of Boiling Water Reactors: Part II-Quantitative Analysis," *Nucl. Sci. Eng*. **93**, 124-136 (1986).

32. D.D.B. van Bragt, Rizwan-uddin and T.H.J.J. van Der Hagen, "Nonlinear Analysis of a Natural Circulation Boiling Water Reactor," *Nuclear Science & Engineering*, **131**, 23-44

(1999).

33. D.D.B. van Bragt, Rizwan-uddin and T.H.J.J. van Der Hagen, **"**Effect of Void Distribution Parameter and Axial Power Profile on BWR Bifurcation Characteristics," to appear in *Nuclear Science & Engineering*.

34. J. March-Leuba, "A Reduced Order Model of Boiling Water Reactor Linear Dynamics," *Nucl. Tech*., **75**, 15-22 (1986).

35. E. Hopf, "Abzweigung Einer Periodischen Losung von Einer Stationaren Losung eines Differential Systems," *Ber. Math.-Phys. Kl. Sachs Acad. Wiss. Leipzig*, **94**, 1-22, and *Ber. Verh. Sachs. Acad. Wiss. Leipzig Math._Nat. Kl*., **95** (1), 3-22, 1942. A translation by L. Howard and N. Koeppel appeared in The Hopf Bifurcation and its Applications, Eds. J.E. Marsden and M. McCracken, Springer-Verlag, Berlin, 1976.

36. J.K. Hale and H. Koçak, Dynamics and Bifurcations, Springer-Verlag, New York (1991).

37. B.D. Hassard, N.D. Kazarinoff and Y.H. Wan, Theory and Applications of Hopf Bifurcation, Cambridge University Press, New York (1981).

38. J. Guckenheimer and P. Holmes, Nonlinear Oscillations, Dynamical Systems, and Bifurcations of Vector Fields, Springer-Verlag, 1983.

39. S. Wiggins, Introduction to Applied Nonlinear Dynamical Systems and Chaos, Springer-Verlag, 1990.

40. A.H. Nayfeh and B. Balachandran, Applied Nonlinear Dynamics: Analytical, Computational, and Experimental Methods, John Wiley, 1995.

41. M. Golubitsky and D.G. Schaeffer, Singularities and Groups in Bifurcation Theory, Springer-Verlag, Applied Math. Sci., Vol. 51 (1984).

42. J. Hale, Theory of Functional Differential Equations, Springer-Verlag, Applied Math. Sci., Vol. 3, (1977).

43. B.D. Hassard, "Numerical Evaluation of Hopf Bifurcation Formulas," Chapter 9 in Dynamics of Nonlinear Systems, V. Hlavacek, Editor, Gordon and Breach (1986).

44. B.D. Hassard, "A Code for Hopf Bifurcation Analysis of Autonomous Delay-Differential Equations," Proc. Oscillation, Bifurcation and Chaos, Canadian Mathematical Society, pp. 447-463 (1987).

45. A. Clausse and R.T. Lahey, "The Analysis of Periodic and Strange Attractors During Density-

Wave Oscillations in Boiling Flows," *Chaos, Solitons, and Fractals,* **1**, 2, 167-178 (1991).

46. N. Takenaka, R.T. Lahey and M.Z. Podowski, "The Analysis of Chaotic Density-Wave Oscillations," *Trans. Am. Nucl. Soc*., **63**, 197-198, 1991.

47. Jean-Luc Achard, D.A. Drew and R. Lahey, "The Analysis of Nonlinear Density-Wave Oscillations in Boiling Channels," *J. Fluid Mech*. **155**, 213-232 (1985).

48. Rizwan-uddin and J.J. Dorning, "Some Nonlinear Dynamics of a Heated Channel," *Nucl. Eng. Des*., **93**, 1-14 (1986). Also see: Rizwan-uddin and J.J. Dorning, "Nonlinear Stability Analysis of Density Wave Oscillations in Nonuniformly Heated Channels," *Trans. Am. Nucl. Soc*., **54**, p. 172 (1987).

49. G.B. Ermentrout, "WINPP: A PC-Based Dynamical System Software Package," Department of Mathematics, University of Pittsburgh (http://www.pitt.edu/~phase/), 1996.